

INFLUENCE OF STRUCTURAL DEFECTS ON THE MAGNETIC PROPERTIES OF MASSIVE AMORPHOUS $\text{Fe}_{60}\text{Co}_{10}\text{Mo}_2\text{W}_x\text{Y}_8\text{B}_{20-x}$ ($x = 1, 2$) ALLOYS PRODUCED WITH THE INJECTION CASTING METHOD

VPLIV STRUKTURNIH NAPAK NA MAGNETNE LASTNOSTI MASIVNE AMORFNE ZLITINE $\text{Fe}_{60}\text{Co}_{10}\text{Mo}_2\text{W}_x\text{Y}_8\text{B}_{20-x}$ ($x = 1, 2$), IZDELANE Z METODO LITJA Z VBRIZGAVANJEM

Joanna Gondro, Katarzyna Bloch, Marcin Nabialek, Sebastian Garus

Institute of Physics, Faculty of Production Engineering and Materials Technology, Czestochowa University of Technology,
Al. Armii Krajowej 19, 42-200 Czestochowa, Poland
j.gondro@wp.pl

Prejem rokopisa – received: 2015-06-30; sprejem za objavo – accepted for publication: 2015-07-29

doi:10.17222/mit.2015.148

This paper presents the results of research pertaining to high-field magnetic properties, in relation to the theory of H. Kronmüller. Studies were performed on bulk amorphous alloys featuring composition $\text{Fe}_{60}\text{Co}_{10}\text{Mo}_2\text{W}_x\text{Y}_8\text{B}_{20-x}$ ($x = 1, 2$). Samples were produced in the form of plates with a thickness of 0.5 mm; they were prepared by injecting the molten alloy into a water-cooled copper mould. The influence of structural defects on the magnetization process was investigated within high magnetic fields known as the area of the approach to ferromagnetic saturation. For the investigated samples, the studies showed that, in the process of magnetization in high magnetic fields, rotation of the magnetization vector was mainly due to the presence of linear defects in the structure, i.e., quasidislocational dipoles. The density of quasidislocational dipoles in a sample with an addition of 1 % W was nearly twice as high as that of an alternative alloy.

Keywords: bulk amorphous alloy, metallic glasses, high magnetic fields, magnetization, structural defects, relaxation

Članek predstavlja rezultate raziskav, ki se nanašajo na visokomagnetne lastnosti, v povezavi s teorijo H. Kronmüllerja. Študije so bile izvedene na masivni amorfnih zlitini s sestavo $\text{Fe}_{60}\text{Co}_{10}\text{Mo}_2\text{W}_x\text{Y}_8\text{B}_{20-x}$ ($x = 1, 2$). Vzorci so bili izdelani v obliki ploščic debeline 0,5 mm, izdelane z vbrizgavanjem staljene zlitine v vodno hlajeno bakreno kokilo. Preiskovan je bil vpliv napak v strukturi na proces magnetizacije v visokomagnetnih poljih, poznanih kot področje približka k feromagnetnemu nasičenju. Za preiskovane vzorce so raziskave pokazale, da pri procesu magnetizacije v visoko magnetnih poljih pride do rotacije magnetnega vektorja predvsem zaradi prisotnosti linearnih napak v strukturi: to so kvazidislokacijski dipoli. Gostota dislokacijskih dipolov v vzorcu, z dodatkom 1 % W, je bila skoraj dvakrat višja kot pa pri drugi zlitini.

Gljučne besede: masivna amorfn zlitina, kovinska stekla, visokomagnetno polje, magnetizacija, napake v strukturi, relaksacija

1 INTRODUCTION

Within the past decade, a group of materials known as ‘bulk amorphous alloys’ have been studied intensely;¹⁻⁴ This interest is associated with their excellent soft-magnetic and mechanical properties, which facilitate their application. The amorphous alloys can be classified into two categories: classic (in the form of thin ribbons with a thickness of up to 100 μm) and bulk amorphous alloys (with a thickness greater than 100 μm). The bulk amorphous alloys are characterised by properties, which are very difficult or even impossible to achieve in the classic, ribbon-shaped, amorphous alloys.^{5,6} The group of bulk amorphous alloys includes: ribbons with a thicknesses of approximately 100 μm , plates and rods with diameters of a few millimetres, and cores that can feature complex shapes.⁷

Although the finished amorphous alloys are in the solid state, the constituent particles are distributed in a chaotic way; their configuration is closer to that of the

liquid state.⁸ These alloys are characterised by a lack of a long-range order and they exist in a metastable state. If a sufficient quantity of energy is delivered to these metastable materials, the crystallisation process will be activated; therefore, this value of energy is called the activation energy. The barriers to their crystallisation, during the rapid-quenching process from the liquid state (10^4 – 10^6 K/s), are mainly their high viscosity and the presence of inclusions within their volumes.

The bulk amorphous alloys consist of more than three elements and they are based mostly on Pd, Zr, Ti, Al, Mg, Fe or Cu. The group with the highest prospects for applications is based on Fe. Given an appropriate composition of this type of alloy, it is possible to obtain a material with a stable structure and excellent magnetic properties – both hard and soft. These properties are often determined by local stresses in the structure, resulting from the existence of structural defects. In the case of crystalline materials, these irregularities are point and linear defects; their counterparts in the amorphous

materials are free volumes and quasidislocational dipoles.

Defects are usually the result of the production process itself, being a by-product of the rapid solidification, "freezing" the structure. The resulting free volumes facilitate short- and long-distance movement of the atoms within the systems of atomic pairs.^{8,9} The free volumes created in a relatively slow solidification process, below the glass transition temperature, have the ability to create cluster systems. These clusters are systems with a low stability and, as a result of the atomic movement, they disintegrate into simpler, two-dimensional systems called quasidislocational dipoles.^{10,11} A direct observation of the structural defects of an amorphous structure is very difficult; therefore, the indirect method is used. This method involves observation and analysis of the initial magnetisation curve, according to the H. Kronmüller theorem.¹² On the basis of the modified Brown micromagnetism theorem¹³, H. Kronmüller showed that structural defects in the ferromagnetic materials with soft magnetic properties are the source of internal stresses, causing a locally inhomogeneous distribution of the magnetisation vector. The presence of these stresses in an amorphous material prevents the achievement of the state of ferromagnetic saturation, even under the influence of a strong magnetic field.¹²

The magnetisation of the amorphous alloys within high magnetic fields, in the so-called "approach to the ferromagnetic saturation" region, could be described using the following Equation (1):⁹

$$\mu_0 M(H) = \mu_0 M_s \left[1 - \frac{a_{1/2}}{(\mu_0 H)^{1/2}} - \frac{a_1}{(\mu_0 H)^1} - \frac{a_2}{(\mu_0 H)^2} \right] + b(\mu_0 H)^{1/2} \quad (1)$$

where:

M_s – spontaneous magnetization; μ_0 – magnetic permeability of a vacuum; H – magnetic field; a_i – directional coefficients of the linear fit (free volumes and linear defects $i = 1/2, 1, 2$); b – directional coefficient of the linear fit.

The b coefficient is calculated on the basis of the spin-wave theorem and connected with the spin-wave stiffness parameter (D_{sp}) with the following relation:^{14–16}

$$b = 3.54 g \mu_0 \mu_B \left(\frac{1}{4\pi D_{sp}} \right)^{3/2} k_B T (g \mu_B)^{1/2} \quad (2)$$

where:

μ_B – Bohr magneton, k_B – Boltzmann constant, g – gyromagnetic coefficient, T – temperature.

The strongest influence on the stresses, connected with the existence of free volumes, is observed for the $a_{1/2}$ coefficient:

$$\frac{a_{1/2}}{(\mu_0 H)^{1/2}} = \mu_0 \frac{3}{20 A_{ex}} \left(\frac{1+r}{1-r} \right)^2 \cdot G^2 \lambda_s^2 (\Delta V)^2 N \left(\frac{2 A_{ex}}{\mu_0 M_s} \right)^{1/2} \frac{1}{(\mu_0 H)^{1/2}} \quad (3)$$

where:

N – volume density of point defects, ΔV – volume change caused by point defects, A_{ex} – exchange constant, r – Poisson number, G – transverse elasticity modulus, λ_s – saturation magnetostriction.

The elements $a_1/\mu_0 H$ and $a_2/(\mu_0 H)^2$ are connected with the linear, elongated agglomerates of free volumes, in which the internal stress field is equivalent to the field created by linear dislocation dipoles with a width of D_{dip} , the effective Burgers vector b_{eff} and the surface density of N . The stresses related to these defects cause a non-collinear distribution of the magnetic moments in their vicinity:¹⁷

$$\frac{a_1}{(\mu_0 H)} = 1.1 \mu_0 \frac{G^2 \lambda_s^2}{(1-V)^2} \frac{N b_{eff}}{M_s^2} D_{dip}^2 \frac{1}{(\mu_0 H)^2} \quad (4)$$

This situation exists, when $l_H^{-1} D_{dip} < 1$, and l_H is the exchange distance given with the following equation:^{18,19}

$$l_H = \left(\frac{2 A_{ex}}{\mu_0 H M_s} \right)^{1/2} \quad (5)$$

In the case where $l_H^{-1} D_{dip} > 1$, the dominant element influencing the magnetisation process, according to Equation (1), is $a_2/(\mu_0 H)^2$; this is described with Equation (6):

$$\frac{a_2}{(\mu_0 H)^2} = 0.456 \mu_0 \frac{G^2 \lambda_s^2}{(1-V)^2} \frac{N b_{eff}}{M_s^2} D_{dip}^2 \frac{1}{(\mu_0 H)^2} \quad (6)$$

In Equation (1), each separate element exerts a major influence on the magnetisation process in the approach to the ferromagnetic saturation region, in strictly defined ranges of the magnetic field. Therefore, it is possible to define the influence of structural defects, inherent in amorphous materials, on the magnetisation process within high magnetic fields. On the basis of "defined" defects, their packing density within the alloy volume can be calculated using Equations (3), (4) and (6).²⁰

2 MATERIALS AND METHODS

In this paper, results of investigations are presented for the samples obtained by injecting liquid alloy into a water-cooled copper die under a protective atmosphere of inert gas (Ar). The manufactured samples were in the form of plates with an approximate width of 10 mm and a thickness of 0.5 mm. The nominal compositions of the investigated alloys, $Fe_{60}Co_{10}Mo_2W_xY_8B_{20-x}$ ($x = 1, 2$), were obtained by weighing high-purity (99.9 %) components.

The structure of the resulting alloys was investigated by means of an X-ray diffractometer. The BRUKER "ADVANCE D8" X-ray diffractometer was equipped with a Cu- K_{α} radiation source. The samples were studied within a 2θ range of $30\text{--}120^{\circ}$ with a measurement step size of 0.02° and an exposure time of 5 s per step. Measurements of magnetization were performed over a magnetic field range of $0\text{--}2$ T using a vibrating sample magnetometer (VSM).

3 RESULTS AND DISCUSSION

X-ray diffraction (XRD) curves for the investigated alloys are presented in **Figure 1**. These curves feature only one broad maximum, as characteristic of amorphous materials.

Static hysteresis loops were found to exhibit shapes typical for ferromagnetic materials, which exhibit soft magnetic properties (**Figure 2**).

The value of the coercive field was obtained from an analysis of the static hysteresis loops, being 8705.57 A/m for the $\text{Fe}_{60}\text{Co}_{10}\text{W}_1\text{Mo}_2\text{Y}_8\text{B}_{19}$ alloy and 4610.88 A/m for $\text{Fe}_{60}\text{Co}_{10}\text{W}_2\text{Mo}_2\text{Y}_8\text{B}_{18}$ (**Figure 3**).

From an analysis of the magnetisation as a function of magnetic-field induction curves, it was found that the magnetisation process in the $\text{Fe}_{60}\text{Co}_{10}\text{W}_1\text{Mo}_2\text{Y}_8\text{B}_{19}$ alloy (**Figures 4 to 6**), where the domain structure is not

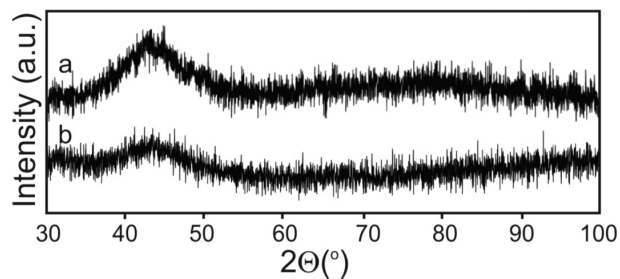


Figure 1: X-ray diffraction patterns for powdered as-quenched samples: a) $\text{Fe}_{60}\text{Co}_{10}\text{W}_1\text{Mo}_2\text{Y}_8\text{B}_{19}$ and b) $\text{Fe}_{60}\text{Co}_{10}\text{W}_2\text{Mo}_2\text{Y}_8\text{B}_{18}$

Slika 1: Rentgenska difrakcija kaljenih vzorcev prahu: a) $\text{Fe}_{60}\text{Co}_{10}\text{W}_1\text{Mo}_2\text{Y}_8\text{B}_{19}$ in b) $\text{Fe}_{60}\text{Co}_{10}\text{W}_2\text{Mo}_2\text{Y}_8\text{B}_{18}$

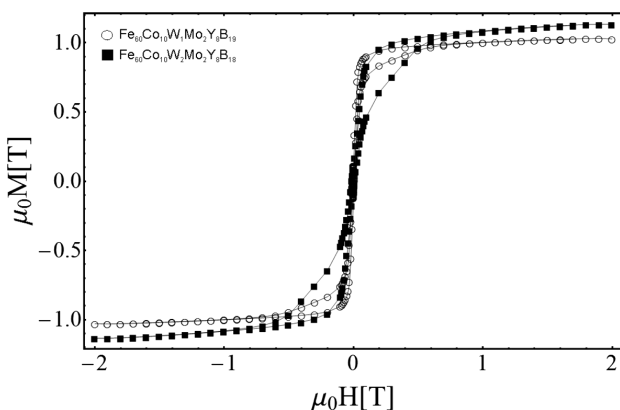


Figure 2: Static hysteresis loops obtained for the investigated alloys

Slika 2: Statične histerezne zanke, dobljene pri preiskovanih zlitinah

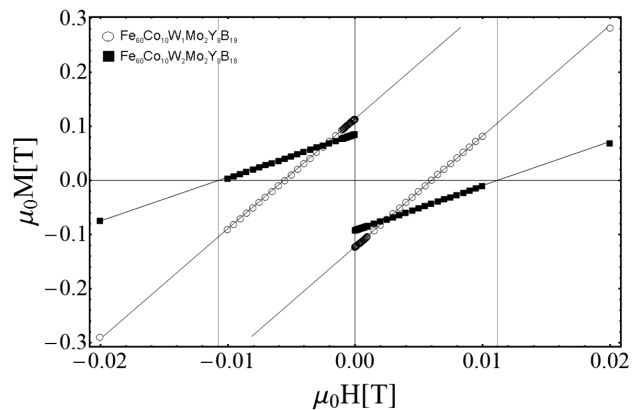


Figure 3: Coercive field obtained from the analysis of the static hysteresis loops for the investigated alloys

Slika 3: Koercitivno polje, dobljeno iz analize statičnih histereznih zank pri preiskovanih zlitinah

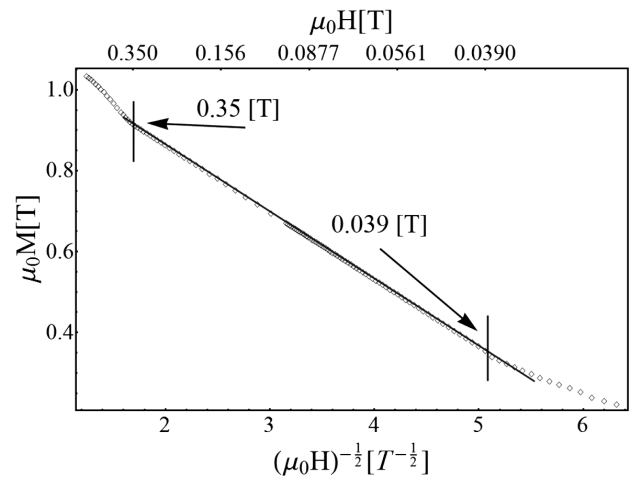


Figure 4: Curves of high-field magnetization as a function of $(\mu_0H)^{-1/2}$, for a plate-shaped sample of $\text{Fe}_{60}\text{Co}_{10}\text{W}_1\text{Mo}_2\text{Y}_8\text{B}_{19}$ alloy

Slika 4: Krivulje visokopoljske magnetizacije kot funkcija $(\mu_0H)^{-1/2}$ pri ploščatih vzorcih iz zlitine $\text{Fe}_{60}\text{Co}_{10}\text{W}_1\text{Mo}_2\text{Y}_8\text{B}_{19}$

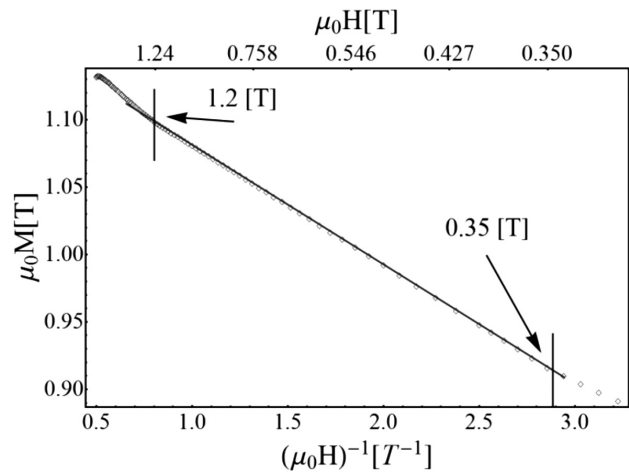


Figure 5: Curves of high-field magnetisation as a function of $(\mu_0H)^{-1}$, for a plate-shaped sample of $\text{Fe}_{60}\text{Co}_{10}\text{W}_1\text{Mo}_2\text{Y}_8\text{B}_{19}$ alloy

Slika 5: Krivulje visokopoljske magnetizacije kot funkcija $(\mu_0H)^{-1}$ pri ploščatih vzorcih iz zlitine $\text{Fe}_{60}\text{Co}_{10}\text{W}_1\text{Mo}_2\text{Y}_8\text{B}_{19}$

Table 1: Results of the analysis of magnetisation as a function of magnetic field to the powers of $^{-1/2}$, $^{-1}$ and $^{1/2}$; spin-wave stiffness parameter D_{spf} and N_{dip} – density of quasislational dipoles

Tabela 1: Rezultati preizkusa magnetizacije kot funkcije magnetnega polja na potenco $^{-1/2}$, $^{-1}$ in $^{1/2}$; parametra vrtilno-valovne togosti D_{spf} in gostote kvazidisllokacijskih dipolov N_{dip}

Composition	$a_{1/2}$ ($\text{T}^{-1/2}$)	a_1 (T^{-1})	b ($\text{T}^{-1/2}$)	D_{spf} (meVnm^2)	N_{dip} (10^{16}m^{-2})
$\text{Fe}_{60}\text{Co}_{10}\text{W}_1\text{Mo}_2\text{Y}_8\text{B}_{19}$	0.166	0.089	0.108	29	51
$\text{Fe}_{60}\text{Co}_{10}\text{W}_2\text{Mo}_2\text{Y}_8\text{B}_{18}$	0.611	0.040	0.085	34	30

present, is influenced by two types of defect: point defects, indicated, in **Figure 4**, by the linear relationship of magnetisation as a function of $(\mu_0 H)^{-1/2}$ over a magnetic field range of 0.039–35 T and linear defects (called quasislational dipoles), indicated, in **Figure 5**, by the linear relationship of magnetisation as a function of $(\mu_0 H)^{-1}$ over a magnetic field range of 0.35–1.2 T. In a strong magnetic field, i.e., greater than 1.2 T, a small increase in the magnetisation is connected with the

dumping of thermally induced spin waves by the strong magnetic field (**Figure 6**).

The high-field magnetisation curves for the $\text{Fe}_{60}\text{Co}_{10}\text{W}_2\text{Mo}_2\text{Y}_8\text{B}_{18}$ alloy are presented in **Figures 7 to 9**. Similarly, in the case of this alloy, the magnetisation process is connected with the rotation of magnetic moments around the point defects (**Figure 7**) and linear defects (**Figure 8**), for which the relationship $l_{\text{H}}^{-1} D_{\text{dip}} < 1$ was fulfilled. The further increase in the magnetisation is

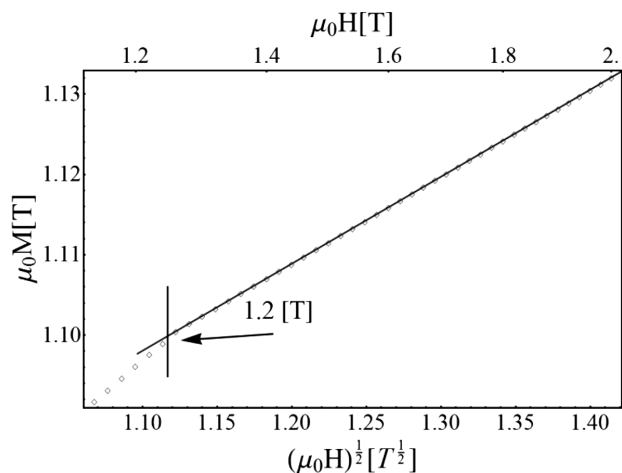


Figure 6: Curves of high-field magnetisation as a function of $(\mu_0 H)^{1/2}$, for a plate-shaped sample of $\text{Fe}_{60}\text{Co}_{10}\text{W}_1\text{Mo}_2\text{Y}_8\text{B}_{19}$ alloy
Slika 6: Krivulje visokopoljske magnetizacije, kot funkcija $(\mu_0 H)^{1/2}$ pri ploščatih vzorcih iz zlitine $\text{Fe}_{60}\text{Co}_{10}\text{W}_1\text{Mo}_2\text{Y}_8\text{B}_{19}$

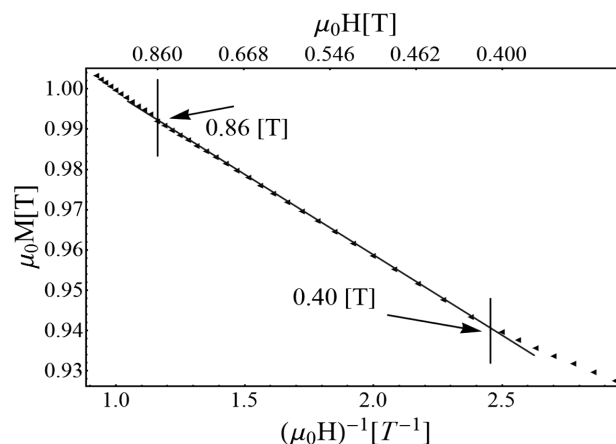


Figure 8: Curves of high-field magnetisation as a function of $(\mu_0 H)^{-1}$, for a plate-shaped sample of $\text{Fe}_{60}\text{Co}_{10}\text{W}_2\text{Mo}_2\text{Y}_8\text{B}_{18}$ alloy
Slika 8: Krivulje visokopoljske magnetizacije, kot funkcija $(\mu_0 H)^{-1}$ pri ploščatih vzorcih iz zlitine $\text{Fe}_{60}\text{Co}_{10}\text{W}_2\text{Mo}_2\text{Y}_8\text{B}_{18}$

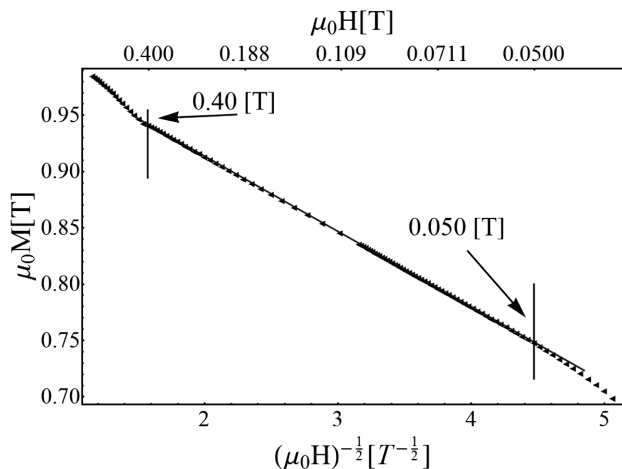


Figure 7: Curves of high-field magnetisation as a function of $(\mu_0 H)^{-1/2}$, for a plate-shaped sample of $\text{Fe}_{60}\text{Co}_{10}\text{W}_2\text{Mo}_2\text{Y}_8\text{B}_{18}$ alloy
Slika 7: Krivulje visokopoljske magnetizacije, kot funkcija $(\mu_0 H)^{-1/2}$ pri ploščatih vzorcih iz zlitine $\text{Fe}_{60}\text{Co}_{10}\text{W}_2\text{Mo}_2\text{Y}_8\text{B}_{18}$

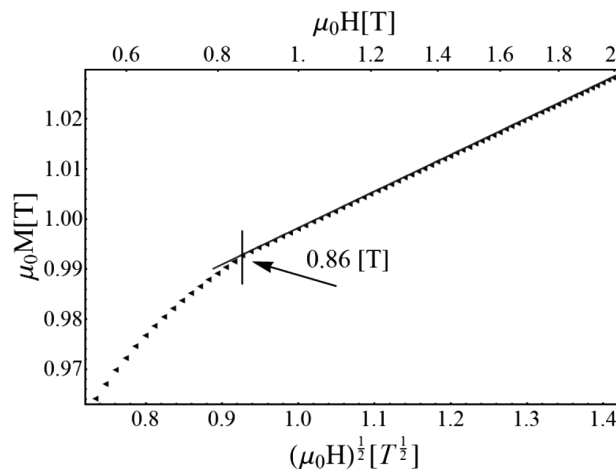


Figure 9: Curves of high-field magnetisation as a function of $(\mu_0 H)^{1/2}$, for a plate-shaped sample of $\text{Fe}_{60}\text{Co}_{10}\text{W}_2\text{Mo}_2\text{Y}_8\text{B}_{18}$ alloy
Slika 9: Krivulje visokopoljske magnetizacije, kot funkcija $(\mu_0 H)^{1/2}$ pri ploščatih vzorcih iz zlitine $\text{Fe}_{60}\text{Co}_{10}\text{W}_2\text{Mo}_2\text{Y}_8\text{B}_{18}$

related with the existence of the Holstein-Primakoff paraprocess (Figure 9).^{21,22}

The parameters obtained from the analysis of the high-field magnetization curves, obtained for both alloys, are presented in Table 1.

4 CONCLUSIONS

During the production process involving bulk amorphous alloys, structural relaxations occur, leading to a more stable structure. This process influences both topological (TSRO) and chemical (CSRO) short-range ordering. Changes in TSRO are irreversible and connected with the decreases in the volume and redistribution of free volumes.²³ As a result, the average distance between the atoms decreases and this, in turn, causes an increase in the atomic packing density.

On the basis of the obtained results of the current investigations, it could be stated that the investigated alloys are amorphous. The value of the coercivity for $\text{Fe}_{60}\text{Co}_{10}\text{W}_2\text{Mo}_2\text{Y}_8\text{B}_{18}$ is half the value for the other alloy.

On the basis of the magnetisation studies, carried out in strong magnetic fields, it was found that for both alloys the magnetisation process was influenced by the presence of point defects and quasidislocational dipoles. Also, the dumping of thermally induced spin waves by the magnetic field (Holstein-Primakoff paraprocess) has an influence on the magnetisation process. In the case of the $\text{Fe}_{60}\text{Co}_{10}\text{W}_2\text{Mo}_2\text{Y}_8\text{B}_{18}$ alloy, both the $a^{1/2}$, and a^1 coefficients are half the equivalent values found for the $\text{Fe}_{60}\text{Co}_{10}\text{W}_1\text{Mo}_2\text{Y}_8\text{B}_{19}$ alloy. Also, the value of the density of the quasidislocational dipoles N_{dip} is almost halved for the alloy with a higher tungsten content. These values indicate a higher atomic packing density in the $\text{Fe}_{60}\text{Co}_{10}\text{W}_2\text{Mo}_2\text{Y}_8\text{B}_{18}$ alloy. The analysis of the high-field magnetisation curves facilitated the calculation of the spin-wave stiffness parameter, D_{spf} , which is connected with the changes in the chemical and topological atomic ordering. The higher value of this parameter for the sample of the $\text{Fe}_{60}\text{Co}_{10}\text{W}_2\text{Mo}_2\text{Y}_8\text{B}_{18}$ alloy indicates a high concentration of magnetic atoms in a given volume and confirms that the alloy has a higher atomic packing density.

On the basis of the performed investigations, it can be stated that an addition of 1 % (by weight) of tungsten, replacing boron, caused a decrease in the number of defects present in the investigated material and an increase in the value of the spin-wave stiffness parameter D_{spf} . This indicates that, during the solidification process of the $\text{Fe}_{60}\text{Co}_{10}\text{W}_2\text{Mo}_2\text{Y}_8\text{B}_{18}$ alloy, structural relaxations caused more atoms to take locally ordered positions. In turn, this led to a decrease in the size of free volumes and an increase in the atomic packing density within the structure.

5 REFERENCES

- 1 T. Thomas, M. R. J. Gibbs, Anisotropy and magnetostriction in metallic glasses, *Journal of Magnetism and Magnetic Materials*, 103 (1992), 97–110, doi:10.1016/0304-8853(92)90242-G
- 2 K. Sobczyk, J. Świerczek, J. Gondro, J. Zbrozarczyk, W. Ciużyńska, J. Olszewski, P. Brągiel, A. Łukiewska, J. Rzącki, M. Nabiałek, Microstructure and some magnetic properties of bulk amorphous $(\text{Fe}_{0.61}\text{Co}_{0.10}\text{Zr}_{0.025}\text{Hf}_{0.025}\text{Ti}_{0.02}\text{W}_{0.02}\text{B}_{0.20})_{100-x}\text{Y}_x$ ($x=0, 2, 3$ or 4) alloys, *Journal of Magnetism and Magnetic Materials*, 324 (2012), 540–549, doi:10.1016/j.jmmm.2011.08.038
- 3 M. Hasiak, K. Sobczyk, J. Zbrozarczyk, W. Ciużyńska, J. Olszewski, M. Nabiałek, J. Kaleta, J. Świerczek, A. Łukiewska, Some magnetic properties of bulk amorphous Fe-Co-Zr-Hf-Ti-W-B-(Y) alloys, *IEEE Transactions on Magnetics*, 11 (2008), 3879–3882, doi:10.1109/TMAG.2008.2002248
- 4 A. Brand, Improving the validity of hyperfine field distributions from magnetic alloys: Part I: Unpolarized source, *Nuclear Instruments and Methods in Physics Research Section B*, B28 (1987), 398–416, doi:10.1016/0168-583X(87)90182-0
- 5 M. Nabiałek, Soft magnetic and microstructural investigation in Fe-based amorphous alloy, *Journal of Alloys and Compounds*, 642 (2015), 98–103, doi:10.1016/j.jallcom.2015.03.250
- 6 J. Olszewski, J. Zbrozarczyk, K. Sobczyk, W. Ciużyńska, P. Brągiel, M. Nabiałek, J. Świerczek, A. Łukiewska, Thermal stability and crystallization of iron and cobalt-based bulk amorphous alloys, *Acta Physica Polonica A*, 114 (2008) 6, 1659–1666
- 7 A. Inoue, Bulk amorphous alloys with soft and hard magnetic properties, *Materials Science and Engineering A*, A226–228 (1997), 357–363, doi:10.1016/S0921-5093(97)80049-4
- 8 H. Kronmüller, Micromagnetism and microstructure of amorphous alloys (invited), *Journal of Applied Physics*, 52 (1981), 1859–1864, doi:10.1063/1.329552
- 9 H. Kronmüller, Magnetization processes and the microstructure in amorphous metals, *Journal de Physique Colloques*, 41 (1980) C8, C8-618-C8-625, doi:10.1051/jphyscol:19808156. jpa-00220256
- 10 H. Kronmüller, J. Ulner, Micromagnetic theory of amorphous ferromagnets, *Journal of Magnetism and Magnetic Materials*, 6 (1977), 52–56, doi:10.1016/0304-8853(77)90073-7
- 11 K. Bloch, M. Nabiałek, The influence of heat treatment on irreversible structural relaxation in bulk amorphous $\text{Fe}_{61}\text{Co}_{10}\text{Ti}_3\text{Y}_6\text{B}_{20}$ alloy, *Acta Physica Polonica A*, 127 (2015) 2, 442–444, doi:10.12693/APhysPolA.127.442
- 12 H. Kronmüller, Micromagnetism in amorphous alloys, *IEEE Transactions on Magnetics*, 15 (1979) 5, 1218–1225, doi:10.1109/TMAG.1979.1060343
- 13 W. F. Brown Jr., *Micromagnetics*, Interscience Tracts on Physics and Astronomy, Interscience Publishers (John Wiley & Sons), New York, London 1963
- 14 O. Kohmoto, High-field magnetization curves of amorphous alloys, *Journal of Applied Physics*, 53 (1982), 7486–7490, doi:10.1063/1.330121
- 15 M. Nabiałek, P. Pietrusiewicz, M. Dośpiał, M. Szota, J. Gondro, K. Gruszka, A. Dobrzańska-Danikiewicz, S. Walters, A. Bukowska, Effect of manufacturing method on the magnetic properties and formation of structural defects in $\text{Fe}_{61}\text{Co}_{10}\text{Y}_8\text{Zr}_1\text{B}_{20}$ amorphous alloy, *Journal of Alloys and Compounds*, 615 (2015), S56–S60, doi:10.1016/j.jallcom.2013.12.236
- 16 M. Nabiałek, M. Dośpiał, M. Szota, P. Pietrusiewicz, Influence of Solidification Speed on Quality and Quantity of Structural Defects in $\text{Fe}_{61}\text{Co}_{10}\text{Zr}_{2.5}\text{Hf}_{2.5}\text{Y}_2\text{W}_2\text{B}_{20}$ Amorphous Alloy, *Materials Science Forum*, 654–656 (2010), 1074–1077, doi:10.4028/www.scientific.net/MSF.654-656.1074
- 17 M. Vázquez, W. Fernengel, H. Kronmüller, Approach to magnetic saturation in rapidly quenched amorphous alloys, *Physica Status Solidi A*, 115 (1989) 2, 547–553, doi:10.1002/pssa.2211150223

- ¹⁸ M. Hischer, R. Reisser, R. Würschum, H. E. Schaefer, H. Kronmüller, Magnetic after-effect and approach to ferromagnetic saturation in nanocrystalline iron, *Journal of Magnetism and Magnetic Materials*, 146 (1995), 117–122, doi:10.1016/0304-8853(94)01643-7
- ¹⁹ N. Lenge, H. Kronmüller, Low temperature magnetization of sputtered amorphous Fe-Ni-B films, *Physica Status Solidi A*, 95 (1986), 621–633, doi:10.1002/pssa.2210950232
- ²⁰ P. Pietrusiewicz, K. Błoch, M. Nabiałek, S. Walters, Influence of 1 % addition of Nb and W on the relaxation process in classical Fe-based amorphous alloys, *Acta Physica Polonica A*, 127 (2015) 2, 397–399, doi:10.12693/APhysPolA.127.397
- ²¹ T. Holstein, H. Primakoff, Field dependence of the intrinsic domain magnetization of a ferromagnet, *Physical Review Letters*, 58 (1940) 12, 1098–1113, doi:10.1103/PhysRev.58.1098
- ²² K. Błoch, M. Nabiałek, Approach to ferromagnetic saturation for the bulk amorphous alloy: $(\text{Fe}_{0.61}\text{Co}_{0.10}\text{Zr}_{0.025}\text{Hf}_{0.025}\text{Ti}_{0.02}\text{W}_{0.02}\text{B}_{0.20})_{97}\text{Y}_3$, *Acta Physica Polonica A*, 127 (2015) 2, 413–414, doi:10.12693/APhysPolA.127.413
- ²³ F. F. Marzo, A. R. Pierna, M. M. Vega, Effect of irreversible structural relaxation on the electrochemical behavior of $\text{Fe}_{78-x}\text{Si}_{13}\text{B}_9\text{Cr}_{(x=3,4,7)}$ amorphous alloys, *Journal of Non-Crystalline Solids*, 329 (2003), 108–114, doi:10.1016/j.jnoncrysol.2003.08.022